

## Original article

### Influence of gold nanoparticles on the immune response to rift valley fever vaccine and related hepatophysiological toxicity, histological, and immunohistochemical alterations

**Background:** Vaccination is a very effective method of stimulating the immune response against infections. Adjuvants are employed to enhance the immune response, but they must be safe, inexpensive, and easy to use. **Objective:** This study aimed to evaluate gold nanoparticles as immune enhancers for rift valley fever vaccine. **Methods:** The rats were divided into four groups (10 each): the negative control group, rats immunized with nonadjuvanted rift valley fever vaccine and the last two rat groups immunized with rift valley fever vaccine combined with 40  $\mu$ M of spherical gold nanoparticles and combined with 40  $\mu$ M of rod-shaped gold nanoparticles, respectively. **Results:** Compared with rats receiving no treatment and rats treated with nonadjuvanted vaccine, rats treated with vaccines combined with gold nanoparticles exhibited toxic biochemical, histological and immunohistochemical changes, as shown by significant elevations in liver enzymatic markers and total bilirubin. The magnitude of the biochemical changes was dependent on the shape of the gold nanoparticles: the elevations in liver enzymatic markers and total bilirubin were greater in the group treated with spherical gold nanoparticles than in the group treated with rod-shaped gold nanoparticles. **Conclusion:** It can be concluded that gold nanoparticles are promising vaccine cellular and humoral immune enhancers/adjuvants via different cytokine pathways.

**Keywords:** gold nanoparticles, rift valley fever virus, adjuvants, histological and immunohistochemical studies.

**Asmaa A. Abo Elqasem,  
Aly F. Mohamed\*.**

Zoology Department,  
Faculty of Science, Al-  
Azhar University (Girls  
Branch) and  
International Center for  
Training and Advanced  
Researches, Cairo, Egypt

**Correspondence:**  
Asmaa A. Abo Elqasem,  
Zoology Department,  
Faculty of Science, Al-  
Azhar University (Girls  
Branch), Cairo, Egypt.  
**Email:**  
asmaamohamed.sci.g  
@azhar.edu.eg

## INTRODUCTION

Vaccination is one of the most important ways to control healthcare costs and stimulate a protective immune response against infection in all countries. Adjuvant carriers can deposit antigens at the injection site, improve their appearance to immune-competent cells, stimulate T cells, improve antigen processing, and increase B cell antibody secretion. In the preparation of antibodies and vaccines against pathogens, nanoparticles (NPs) are used as carriers and adjuvants.<sup>1,2</sup> NPs interact with the immune system and modulate its activity, resulting in immune stimulation, and have promising medical applications. These modulating effects may be beneficial or harmful.<sup>3,4</sup> Gold nanoparticles (AuNPs) have the potential to be a useful tool in the development of successful vaccines against infectious diseases.<sup>5</sup> AuNPs penetrate macrophages through receptor-mediated endocytosis and are found primarily in lysosomes and the perinuclear space, depending on their size and shape.<sup>6</sup>

The Rift Valley fever virus (RVFV), a member of the genus Phlebovirus in the Bunyaviridae family, causes Rift Valley fever (RVF). In the Arabian Peninsula and Sub-Saharan Africa, RVFV is a mosquito-borne zoonotic pathogen that causes serious outbreaks in humans and livestock. Fever is a symptom of human diseases, which may contribute to retinitis, encephalitis, hemorrhagic fever, and occasionally death.<sup>7</sup> RVFV can be detected using a quantitative reverse transcription polymerase chain reaction (qRT-PCR) or an enzyme-linked immunosorbent assay that detects genomic segments (L, M, S)<sup>8</sup> or surface and non-structural viral proteins<sup>9</sup>, respectively. These tests have a high sensitivity and specificity, but they necessitate the transport of unknown samples from the field to a laboratory, which increases the risk of virus transmission. Zaher *et al.*<sup>10</sup> used unmodified gold nanoparticles (AuNPs) that change color in the presence of RVFV RNA to create a prototype point-of-care diagnostic test specific for RVFV detection, resulting in a simple but sensitive assay. The nanogold assay yields qualitative results that

demonstrate the presence of RVFV RNA in various sample types. With a detection limit of 10 RNA copies/reaction, the assay demonstrated high accuracy and specificity, comparable to quantitative reverse transcription polymerase chain reaction. The assay result could be determined in 30 minutes without the use of any special detection equipment. To protect ruminant populations, three approved veterinary vaccines against RVFV are used: inactivated virus vaccines, live attenuated virus vaccines, and alternative virus vaccines (Clone-13 live and MP-12 live) (OIE, 2015). In the beginning, formalin was used to suppress the virus in mice.<sup>11</sup> Beta-propiolactone (PL) is also commonly used in the development of viral vaccines as inactivating reagent.<sup>12</sup> Nearly 100 adjuvants are currently available or in production for approximately 400 vaccines.<sup>13</sup> AuNPs are a popular antigen carrier used in vaccination and immunization.<sup>14</sup> AuNPs are commonly used in biomedical research due to their unique physicochemical properties, ease of preparation, and low toxicity.<sup>15</sup> We conducted this study to test the activity of spherical and rod-shaped AuNPs as immune enhancers of RVF vaccine.

## METHODS

### Cell culture

Buffalo green monkey cells (Vero) were kindly provided by the cell culture department, VACSERA, Giza, Egypt. The cell line was maintained according to the methods of Abdel-Gaied *et al.*<sup>16</sup> and dispensed in TC plates and TC flasks (SPL-Korea) at  $2 \times 10^5$  cells/ml.

### RVFV strain

RVFV strain Menya/Sheep/258 was kindly provided by Dr. El Karamany, Former-G.M. of the research and development sector, VACSERA, Egypt. The infectivity titer was  $7.5 \log_{10}$  /ml. RVFV seed stock was prepared according to the method of El-Karamany *et al.*<sup>17</sup>

### Inactivation of RVFV

RVFV was inactivated by  $\beta$ PL (0.0035 M) supplied by Sigma-Aldrich (St. Louis, MO, USA).  $\beta$ PL-treated RVFV was incubated at 37°C for 2 h with continuous stirring. Samples were collected at 15-min intervals to evaluate the inactivation potential of  $\beta$ PL.

### AuNPs

Spherical and rod-shaped AuNPs were purchased from Nanotech Company (6<sup>th</sup> October City, Giza, Egypt) at 1 mM final concentration and 20 nm size.

AuNPs were prepared at a final concentration of 40  $\mu$ M.

### Laboratory animals

Forty male albino rats (body weight 75-80 g) were supplied from Theodore Bilharz Research Institute, Giza, Egypt. The rats were housed in both STST cages at VACSERA under standard breeding conditions and supplied with dry food and tap water, at a 12 h light/12 h dark cycle and a temperature of 25 °C.

### Study design

The rats were randomly divided into four groups of 10 each: the negative control (NC) group, rats immunized with nonadjuvanted RVF vaccine (the Vac group), rats immunized with RVF vaccine combined with 40  $\mu$ M of spherical AuNPs (the AuNP-S group), and rats immunized with RVF vaccine combined with 40  $\mu$ M of rod-shaped AuNPs (the AuNP-R group).

### Immune sera

Blood samples were collected from the retro-orbital plexus of the eye. The samples were kept at 37°C for 30 min for blood coagulation and then kept overnight at 4°C for retraction of the clot. The samples were then centrifuged for 15 min at 3500 rpm in a cold centrifuge (Jouan-ki22-Franc). Sera were removed in empty tubes and recentrifuged for another 10 min to remove any remaining blood clots and red blood cells. The collected sera were aliquoted and stored at -80 °C until use.<sup>18</sup>

### Biochemical analysis

Serum samples from the immunized groups and NCs were processed for evaluation of liver function according to measurements of aspartate aminotransferase (AST), alanine aminotransferase (ALT), and total serum bilirubin (TB) using a standard colorimetric kit following the manufacturer's protocol (Biovision, Mountain View, CA, USA).<sup>19</sup>

### Immunological studies: cytokine evaluation

The serum concentration of TNF- $\alpha$  was determined by direct enzyme-linked immunosorbent assay according to the method of Brouckaert *et al.*<sup>20</sup>

### Statistical analysis

All results were expressed as means  $\pm$  SD. Statistical analysis was performed by one-way analysis of variance according to the method of Dawson and Trapp<sup>21</sup> using Statistical Package for the Social Sciences software version 25.

### Histological and immunohistochemical studies

Fresh specimens of liver were taken from the control and treated groups. The specimens were fixed in 10% formal saline neutral buffer, washed, dehydrated in increasing concentrations of alcohol, cleared in xylene, and embedded in paraffin wax. Sections were prepared at 5- $\mu$ m thickness and stained with hematoxylin and eosin (H&E) for histological studies according to the method of Drury and Wallington.<sup>22</sup> Another set of slides was processed for detection of caspase 9 and CD68 as immune markers according to the method of Tan *et al.*<sup>23</sup>

## RESULTS

### Inactivation of RVFV

RVFV seed stock prepared in the Vero cell line was inactivated using 0.0035 M of  $\beta$ PL. Inactivation kinetics was determined relative to time (Fig. 1). RVFV was completely inactivated within 2 h after  $\beta$ PL treatment with a mean depletion of virus infectivity titer on the order of 1.2  $\log_{10}$ /15 min.

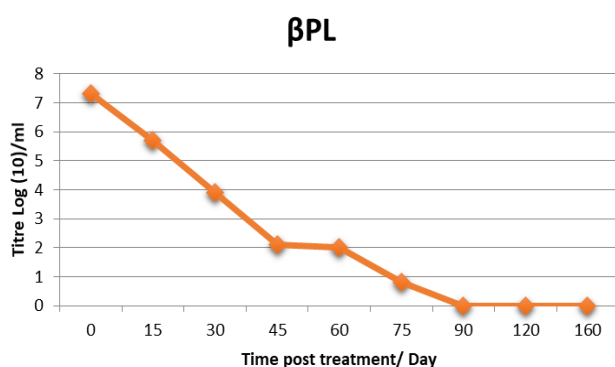


**Figure 1.** Inactivation kinetics of RVFV post treatment with  $\beta$ PL to time.

### Biochemical analysis

Compared with rats receiving no treatment (the NC group) and rats treated with nonadjuvanted vaccine (the Vac group), rats treated with vaccines combined with AuNPs exhibited toxic biochemical changes, as shown by significant elevations in liver enzymatic markers (ALT and AST) and TB ( $P < 0.05$ ) after vaccination in the AuNP-S and AuNP-R groups (Figs. 2–4). The magnitude of the biochemical changes was dependent on the shape of the gold NPs: the elevations in ALT, AST, and TB were greater in the group treated with AuNP-S (spherical NPs) than in the group treated with AuNP-R (rod-shaped NPs). The elevations in ALT,

AST, and TB peaked on day 45 after vaccination and then declined. The biochemical changes were indicative of damage to the plasmalemma of the hepatocytes, resulting in leakage of the enzymes in the liver.

### Immunological results

Levels of TNF- $\alpha$  as a proinflammatory marker were detected on day 8 after vaccination and were significantly elevated ( $P < 0.05$ ) in the AuNP-S and AuNP-R groups (Fig. 5). The elevation was significantly greater in the AuNP-R group than in the AuNP-S group and was significantly reduced on days 60 and 95.

### Histological and immunohistochemical changes in liver tissue

#### Histological studies

H&E stain was used to detect hepatic cellular changes. The NC group showed normal hepatic architecture; the hepatic lobule structure of the liver tissue was normal and the central vein was visible. The hepatocytes were arranged radially around the central vein, the structure of the hepatic sinus was clear, and there were no pathological changes (Fig. 6A). In contrast, the normal lobular structure of the liver tissue was changed in all treated rat groups; the greatest effect was detected in the AuNP-R group. There was a large amount of congestion in some hepatic sinuses and the central vein of the liver, and the hepatic sinus was clearly dilated. A large number of inflammatory cells were infiltrated, and the number of Kupffer cells was increased. Some hepatocytes showed dense cytoplasm and dark nuclei, and others showed vacuolated cytoplasm. There were numerous apoptotic figures (pyknosis and karyorrhexis), and some binucleated cells were observed (Fig. 6B–D).

#### Immunohistochemical studies

Immunohistochemical staining of prepared slides for detection of caspase 9 apoptosis was scored as (–) for normal sections in the NC group, (+3) moderate in the Vac group, (+2) mild in the AuNP-S group, and (+4) highly positive in the AuNP-R group (Fig. 7A–D).

CD68, a widely used monocyte/macrophage lineage marker, was positive in all treated groups and showed a weak positive or negative reaction in the NC group (Figure 8A–D).

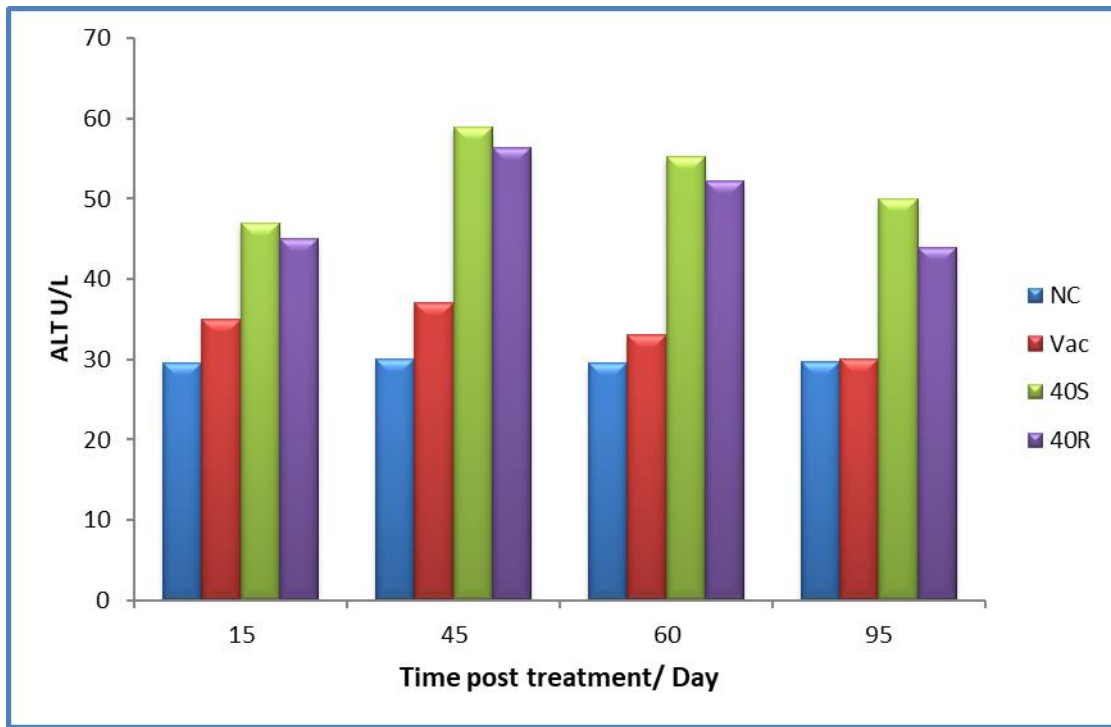


Figure 2. Effect of non-adjuvanted (Vac) and AuNPs adjuvanted vaccine on the activity of ALT.

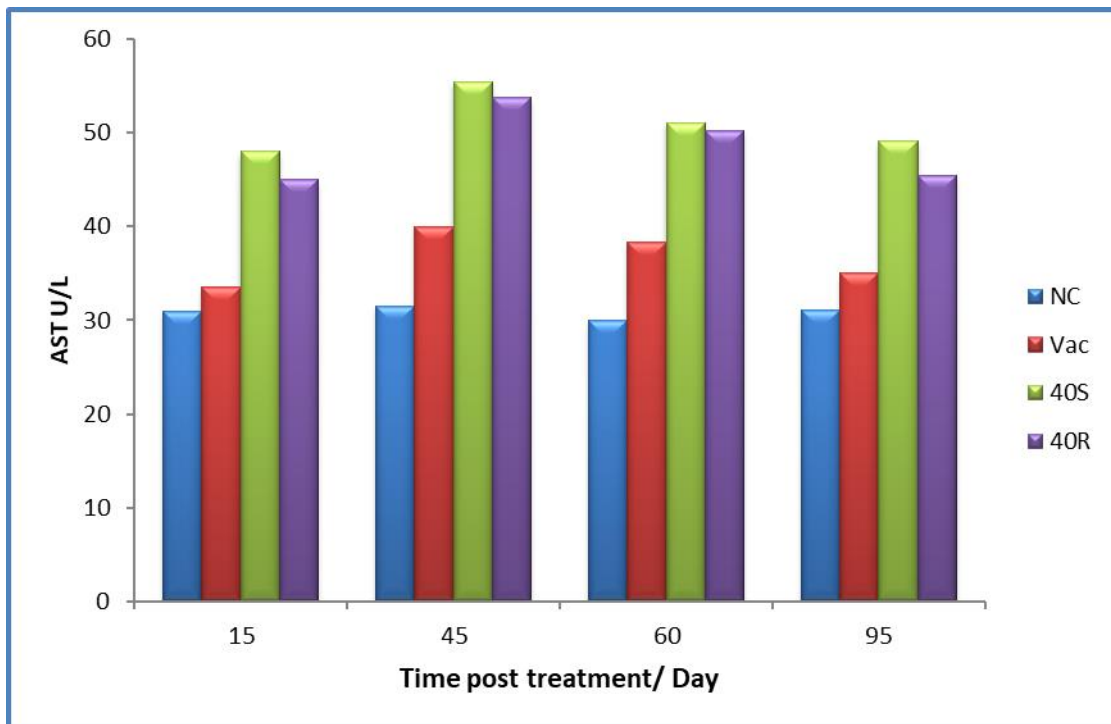
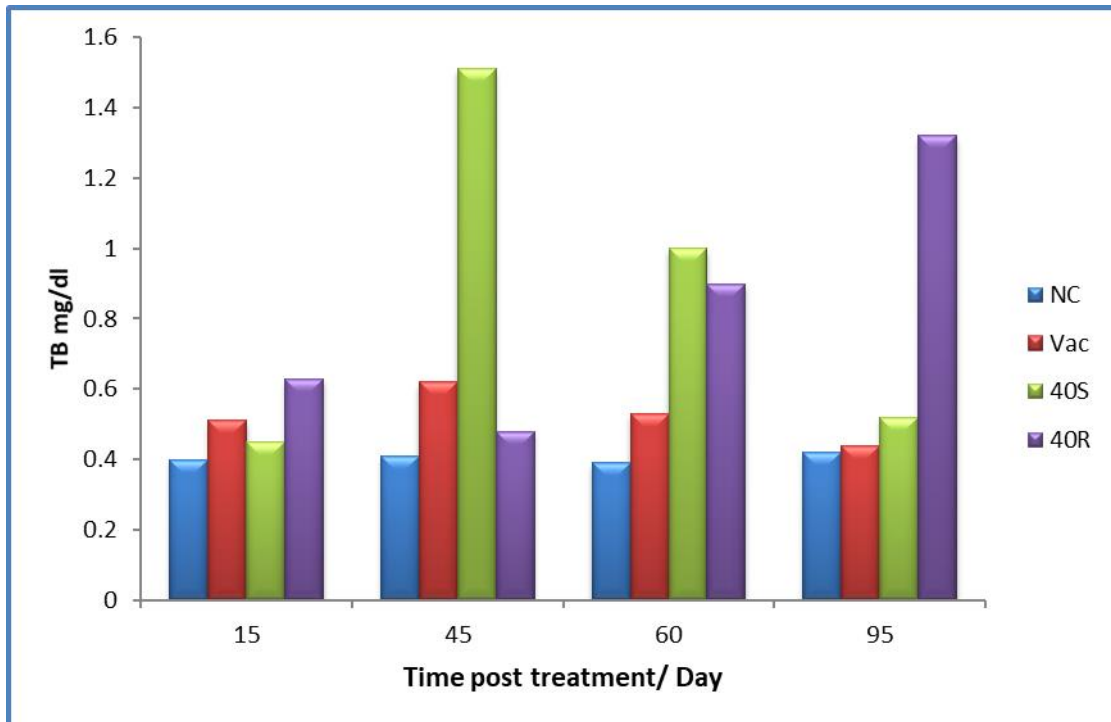
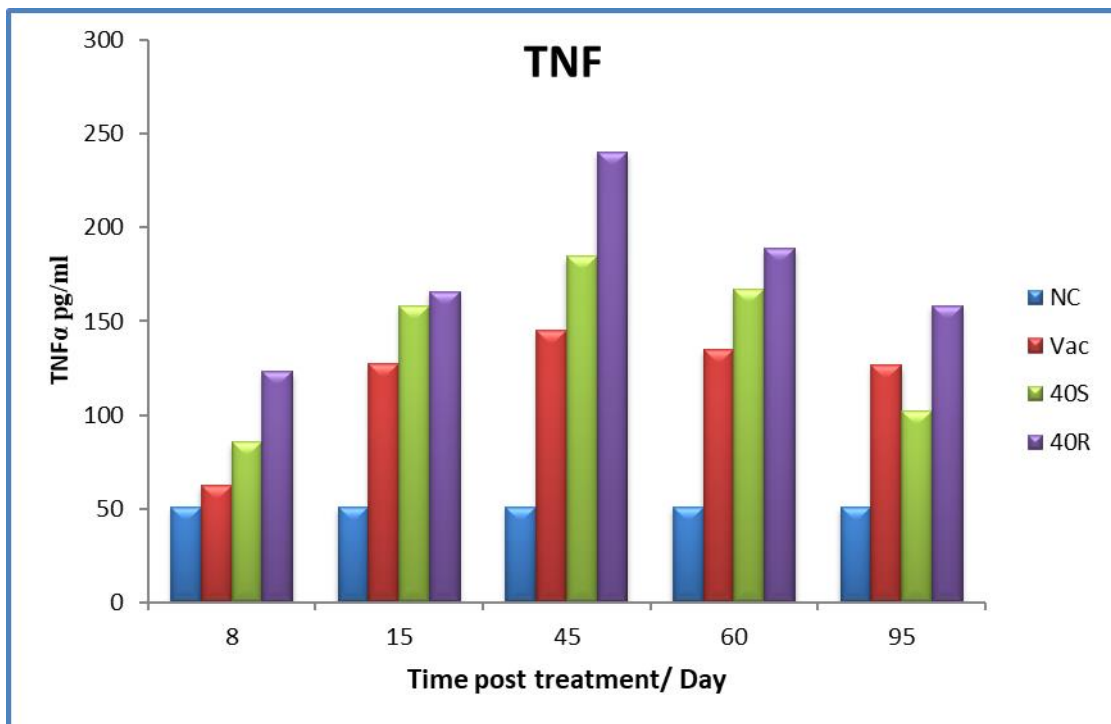


Figure 3. Effect of non-adjuvanted (Vac) and AuNPs adjuvanted vaccine on the activity of AST.



**Figure 4.** Effect of non-adjuvanted (Vac) and AuNPs adjuvanted vaccine on the activity of TB.



**Figure 5.** Effect of Vac (nonadjuvanted group), AuNPs (S&R) (adjuvanted groups) on TNF- $\alpha$  level.

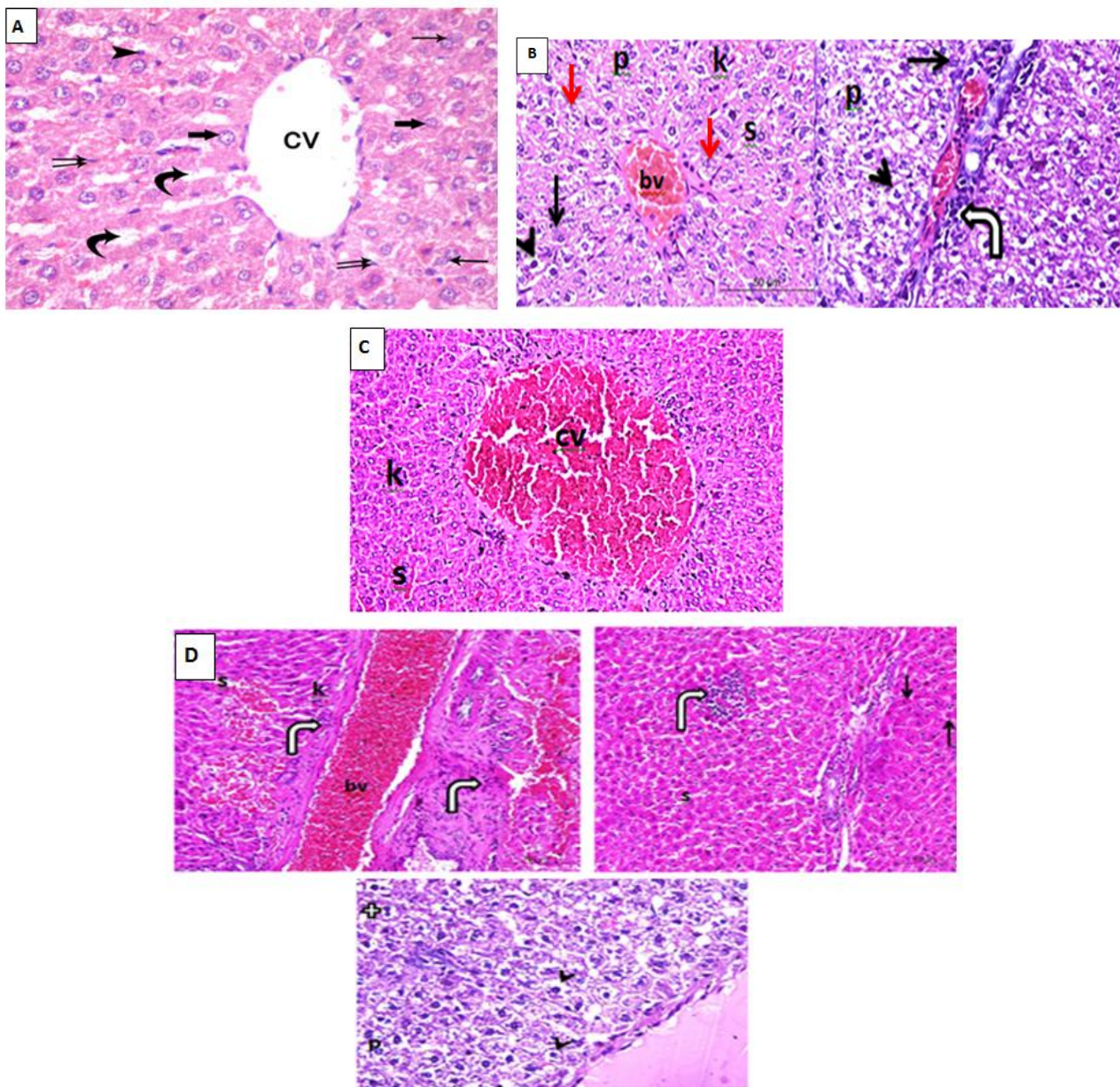


**Figure 6.** (A) Photomicrograph of rat liver of NC group showing, normal hepatocytes (rounded or polyhedral in shape) contain central rounded vesicular nuclei (thick arrows) and sinusoids (curved arrows). Kupffer cells (arrow head) lining sinusoids, few cells are binucleated (thin arrows) and endothelial (double arrows) cells lining are noticed between the hepatocyte plates (H & E stain X 400). (B): Photomicrograph of rat liver of Vac group showing congested blood vessel with RBCs (bv) and dilated blood sinusoids (s). There are numerous apoptotic figures (pyknosis; p and karyorrhexis; red arrows). Hepatocytes show cytoplasmic vacuolation (arrow head) and Kupffer cells (k) are increased in number. There is inflammatory cell infiltration (bent arrow) in the periportal area. Some hepatocytes are with dense cytoplasm and dark nuclei (black arrow) (H&E, X400). (C): Photomicrograph of rat liver of 40S group showing the central vein (cv) and sinusoids (s) are congested with RBCs. The Kupffer cells (k) are increased in number (H&E X400). (D): Photomicrograph of rat liver of 40R group, showing, inflammatory cell infiltration (bent arrow), congested blood vessels (bv), dilated blood sinusoids (s) with increasing number of Kupffer cells (k). Some hepatocytes are with dense cytoplasm and dark nuclei (arrow). Hepatocytes show vacuolated cytoplasm (arrow head), pyknotic nuclei (p) and few hepatocytes are binucleated (plus) (H&E X400).

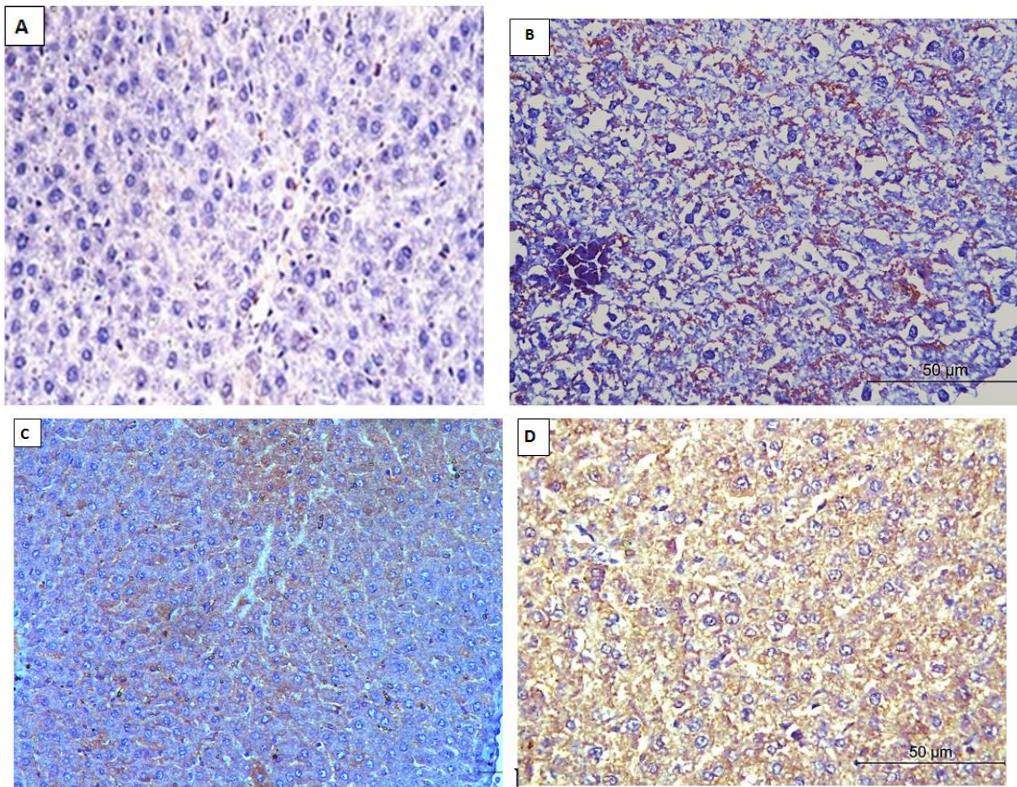


**Figure 7.** (A): Immunohistochemical staining of caspase 9 in liver tissues of NC group, (B): Immunohistochemical staining of caspase 9 in liver tissues of Vac group showed moderate cytoplasmic caspase 9 positivity (+++), (C): Immunohistochemical staining of caspase 9 in liver tissues of 40S group showed mild caspase 9 positivity (++), (D): Immunohistochemical staining of caspase 9 in liver tissues of 40R group showed highly positive (++++) for caspase 9.

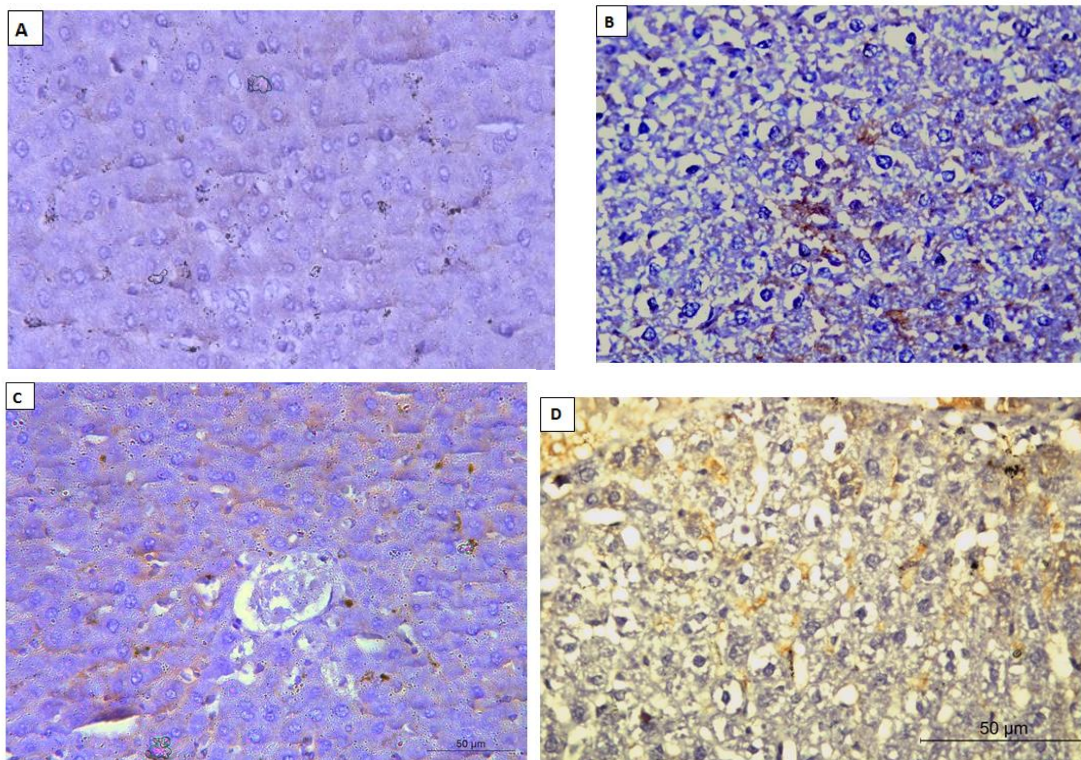


**Figure 8.** (A): Immunohistochemical staining of CD68 in liver tissues of NC group showed weak positive or negative reaction. (B): Immunohistochemical staining of CD68 in liver tissues of Vac group mild positive reaction. (C): Immunohistochemical staining of CD68 in liver tissues of 40S group moderate positive reaction. (D): Immunohistochemical staining of CD68 in liver tissues of 40R group strong positive reaction.

## **DISCUSSION**

Because of their promising chemical and physical properties, AuNPs have piqued researchers' interest in recent years. AuNPs are noncorrosive and, depending on their size and shape, have optical, electronic, and biological properties that have made them useful in a variety of biomedical applications. They have been found to boost immunity.<sup>24</sup> Gold nanospheres, nanorods, nanobelts, nanocages, nanoprisms, and nanostars are some of the shapes that AuNPs can be made in.<sup>25</sup> The interaction of AuNPs with immune cells is extremely important. AuNPs can also be used for immunomodulation and targeted drug delivery.<sup>26</sup>

Nanoparticles (NPs) are perfect for delivering antigens, acting as adjuvant platforms, and mimicking viral structures, and they play a big role in vaccine development. In this study we used AuNPs as enhancers to maximize the immune response to RVF vaccine and preparation of inactivated vaccine was performed using  $\beta$ PL. Within 2 hours of treatment, RVFV was completely inactivated, and the vaccine potency (ED50) was 0.0163 ml, which was in line with WHO recommendations that the ED50 be less than 0.02 ml and Soliman et al.<sup>27</sup> findings. In previous studies Al-Olayan et al.<sup>28</sup> reported that  $\beta$ PL had higher vaccine potency than formalin and ascorbic acid inactivants. This was due to  $\beta$ PL minimal effect on the viral epitope configurations that are responsible for antigenicity, as well as the fact that  $\beta$ PL had no harmful influences on the immune response. Emarat et al.<sup>29</sup> also showed that  $\beta$ PL rapidly inactivated rabies virus within 2 hours, with a depletion rate of 1.8 log<sub>10</sub>/15 min and an ED50 of >2.5 IU/dose, as recommended by WHO.

The use of AuNPs has been linked to liver toxicity and injury, as evidenced by elevated serum ALT and AST levels. Hepatocytes produce these enzymes, which are released into the bloodstream following hepatocellular injury and cholestasis. In our study, the levels of these enzymes were higher in the groups receiving vaccines combined with AuNPs than in the NC group. ALT, AST, and TB activities were more elevated after administration of AuNP-R than after administration of nonadjuvanted vaccine or AuNP-S. Other researchers found elevated liver enzymes after being exposed to AuNP.<sup>30</sup> In another research El Sayed and Mohamed<sup>31</sup> found that the degenerative effect of AuNPs on liver cells significantly increased serum levels of ALT and AST in rats treated with 20  $\mu$ M of spherical and 40  $\mu$ M of rod-shaped AuNPs. In addition, when 10 and 50 nM AuNPs were administered, AST levels increased when compared

to controls.<sup>32</sup> Similarly, AST and ALT levels were significantly higher in animals receiving AuNPs compared to the control group two days after intervention, according to Doudi and Setorki.<sup>33</sup> In the current study TNF- $\alpha$  levels were significantly higher in all treated groups on day 8 compared to the NC group, and significantly lower on days 60 and 95 ( $P < 0.05$ ). The highest TNF- $\alpha$  level was detected after administration of AuNPs-R compared with AuNP-S and nonadjuvanted vaccine. Large amounts of TNF- $\alpha$  were secreted in response to a wide variety of inflammatory stimuli, suggesting a potential role for this cytokine in the increased activation of the peripheral immune system. In accordance with the current findings, Kenichi et al.<sup>34</sup> concluded that rod-shaped AuNPs uptake into cells was as effective as spherical or cubical AuNPs uptake and released significant amounts of inflammatory cytokines such as TNF- $\alpha$ , IL-6, IL-12, IL-10, and granulocyte macrophage colony-stimulating factor (GM-CSF). When rabbits were immunized with 50  $\mu$ g of the HIV-1 Gag p17 peptide conjugated to 2-nm gold glycol-NPs, the proliferation of HIV-specific CD4+ and CD8+ T cells increased and secretion of the highly functional TNF- $\alpha$  and IL-1 $\beta$  cytokines was induced as compared with administration of the unconjugated peptide.<sup>35</sup> AuNPs combined with CpG ODNs considerably enhanced the intracellular penetration of NPs into macrophages and the secretion of the proinflammatory cytokines TNF- $\alpha$  and IL-6, according to Wei et al.<sup>36</sup> Stone et al.<sup>37</sup> investigated the relationship between NP size and shape and immune response. Liu et al.<sup>38</sup> reported that NPs had a low cytotoxic effect on immune cells but significantly stimulated the release of TNF- $\alpha$ , which is essential in the removal of abnormal cells. In accordance with our findings, Bastús et al.<sup>39</sup> found that AuNPs enhanced the induction of proinflammatory cytokines such as TNF- $\alpha$ , IL-1, and IL-6 in macrophages. Malaczewska<sup>40</sup> found that mice given AuNPs orally had increased phagocyte activity and some changes in lymphocyte phenotypes, including a higher percentage of B and CD4+/CD8+ double-positive T cells. The lowest dose increased the synthesis of the proinflammatory cytokines IL-1, IL-2, IL-6, and TNF- $\alpha$ , and had a proinflammatory or immune-stimulating effect. PVP-AuNPs stimulated the synthesis of proinflammatory TNF- $\alpha$ , according to a recent study.<sup>41</sup> TNF- $\alpha$  and IL-6 are cytokines produced by macrophages that affect the systemic inflammatory state.<sup>42</sup> The current study's histological findings largely corroborate the results of biochemical and immunological tests. When compared to the NC

group, the groups receiving nonadjuvanted vaccines and vaccines combined with AuNPs had a lot of histological changes in their liver tissues. After receiving 40  $\mu$ M of AuNP-RVF vaccine, damaged tissues seemed to return to their usual pattern. Histological changes included large numbers of infiltrated inflammatory cells. Guo et al<sup>43</sup> found that giving mice NPs intravenously caused hepatic, renal, and pulmonary inflammation, implying that NPs have their own mechanisms for causing peripheral inflammation. The activation of Kupffer cells resulted in an increase in the number of Kupffer cells in our study. The activation of Kupffer cells has been linked to the toxic potential of AuNPs.<sup>44</sup> Hepatic sinuses and central vein congestion were also caused by the administration of AuNPs. Binucleated cells which found in our study, indicating the regeneration process, as stated by Abdelhalim and Jarrar.<sup>45</sup> Also dense cytoplasm, dark nuclei, and vacuolated cytoplasm were found in some hepatocytes, which may suggest AuNP-induced acute and subacute liver injury. There were a lot of apoptotic figures as well (pyknosis and karyorrhexis). These observed changes were confirmed by Patlolla et al,<sup>46</sup> who stated that as compared to the NC, uncoated and PEG-coated AuNPs caused major morphological changes, such as damage to the central vein; vacuolation in hepatocytes, pyknosis, or karyomegaly; and condensed nuclei of hepatocytes and necrosis. Hepatocyte swelling can be caused by disruptions in membrane function caused by AuNPs, resulting in a large influx of water and Na<sup>+</sup>, as well as leakage of lysosomal hydrolytic enzymes, cytoplasmic degeneration, and macromolecular crowding.<sup>47</sup> Ibrahim et al<sup>48</sup> concluded that the histopathological changes in the liver of AuNPs-treated mice consisted of steatosis, micro- and macrovesicles, cytoplasmic degeneration, necrotic foci, activation of Kupffer cells, hemorrhage, and infiltration of inflammatory cells were similar to our findings. Macrophages and dendritic cells absorbed more nanorods, resulting in increased IL-1 $\beta$  and TNF- $\alpha$  output.<sup>49</sup> In line with our findings, Doudi and Setorki<sup>33</sup> showed that spherical AuNPs caused significant changes in the histopathology of liver hepatic damage and the aggregation of basophilic cells around central vein tissues in all treated groups. Another study found that after receiving AuNPs, which have direct effects on liver function, the liver could be slightly impaired.<sup>32</sup> Hwang et al<sup>50</sup> also published research on healthy and impaired rodent livers during AuNPs-induced hepatotoxicity. Cloudy swelling, vacuolar

degeneration, hyaline droplets and casts, karyorrhexis, and karyolysis were all observed after exposure to AuNP doses. Hepatocyte swelling may also be caused by a malfunction of the cell membrane caused by the large influx of water and Na<sup>+</sup> caused by AuNPs.<sup>51</sup> The pathological changes are related to the time between doses: AuNPs administered every 48 hours demonstrated possible therapeutic benefits without toxicity, while AuNPs administered every 24 hours caused significant parenchymal changes, leukocyte infiltration and cell necrosis.<sup>52</sup> Citrate- and pentapeptide-coated AuNPs (20 nm, 700 g/kg) were rapidly extracted from the bloodstream and accumulated primarily in the liver after injection in rats.<sup>53</sup> A previous study proposed that silymarin-coated AuNPs could be used to treat CCl<sub>4</sub>-induced liver injury and cirrhosis.<sup>54</sup> In our study, immunohistochemical staining of liver sections for detection of caspase 9 apoptosis in NC group was rated as (-), (+3) moderate in the Vac group, (+2) mild in the AuNP-S group, and (+4) strongly positive in the AuNP-R group. These results matched those of Baharara et al<sup>55</sup>, who looked at apoptosis in HaCaT cells induced by PEG-decorated rod-shaped AuNPs and mercaptopropylsulfonate (MPS)-decorated spherical AuNPs. As a result, hexagonal and rod-shaped AuNPs seem to be more likely to cause apoptosis than spherical AuNPs. In Calu-3 epithelial cells, triangular, circular, and hexagonal AuNPs caused higher levels of reactive oxygen species and proapoptotic markers, such as caspase 3 and caspase 9, according to Tian et al.<sup>56</sup> AuNPs induced apoptosis in MCF-7 breast cancer cells through the p53, bax/bcl-2, and caspase pathways (caspase 3 and 9).<sup>57</sup> According to another study, quercetin AuNP enhanced caspase activation (caspase 3 and 9).<sup>58</sup> PEG-coated AuNPs induced acute inflammation and neutrophil influx in the mouse liver, and the percentage of cells undergoing apoptosis in the liver increased on day 7 after treatment.<sup>59</sup> Caspase 9 acts as an initiator caspase that is activated by death-inducing tumor necrosis family receptors and cytochrome C, both of which are involved in immune and apoptosis signaling.<sup>60</sup> In a variety of pathophysiological settings, apoptosis, or programmed cell death, is a critical activity in mammalian cells. It is in charge of getting rid of unwanted cells.<sup>61</sup> CD68 was found to be positive in all of the treated groups in the current study: it was mildly positive in the Vac group, moderately positive in the 40 AuNP-S group, and strongly positive in the AuNP-R group. The increase in CD68 in the treated groups' serum

explained the increase in TNF- $\alpha$  level. This may be because the nanorods were targeted to the tissues at the same rate as the nanospheres, and Alfranca et al.<sup>62</sup> came to the same conclusion. The induction of TNF- $\alpha$  may be related to the curvature of the sphere; the elongated nanorods have a larger surface area in contact with the surface of the endothelial cells, so more of the antibodies that coat the nanorod will attach to receptors on the surface of endothelial cells, resulting in more efficient cell adhesion and a greater impact on the target tissues.<sup>63</sup> Rod AuNPs were more easily taken up by tumor cells, resulting in particle distribution in the tumour.<sup>64</sup> Bartucci et al.<sup>65</sup> corroborated these observations. Previous studies have shown that AuNP administration causes a mild acute hepatic inflammatory response and apoptosis.<sup>59</sup> Different kinds of NPs are used as delivery mechanisms, and they induce alterations in macrophage phenotypes that affect the disease's progression. By inhibiting regulatory pathways activated by macrophages, lipids and polymeric NPs as RNAi vectors can have therapeutic effects.<sup>66</sup> Adult albino rats exposed to AuNPs for a long time developed histological changes, with an immunohistochemical analysis revealing a substantial increase in the number of CD68-positive cells.<sup>67</sup>

## CONCLUSION

AuNPs are promising vaccine cellular and humoral immune enhancers/adjuvants via different cytokine pathways. The immune response depends on the shape of the AuNPs, which influences the activation of dendritic and other antigen-presenting cells. For a better safety measure, further long-term studies involving several apoptotic signaling pathways and other biomarkers based on transcriptomics and proteomics should be conducted.

## ACKNOWLEDGEMENTS

Authors thank the VACSERA lab scientific and technical staff for caring for animals and making specimens available for processing.

## FUNDING SOURCES

This research did not receive any specific grant from funding agencies in the public, commercial, or not-for-profit sectors.

## CONFLICT OF INTEREST

The authors declare that there is no Conflict of interest. The authors alone are responsible for the content and writing of this article.

## ETHICAL USE OF ANIMALS IN RESEARCH

All applicable international, national, and institutional guidelines<sup>65</sup> for the care and use of animals were followed. We respected the welfare of animals, and excluded situations when animals were in pain.

## REFERENCES

1. **PATI R, SHEVTSOV M, SONAWANE A.** Nanoparticle vaccines against infectious diseases. *Front Immunol.* 2018;9:2224.
2. **HESS KL, MEDINTZ IL, JEWELL CM.** Designing inorganic nanomaterials for vaccines and immunotherapies. *Nano Today.* 2019;27:73-98.
3. **FREY M, BOBBALA S, KARABIN N, SCOTT E.** Influences of nanocarrier morphology on therapeutic immunomodulation. *Nanomedicine.* 2018; 13(14): 795-811.
4. **KELLY HG, KENT SJ, WHEATLEY AK.** Immunological basis for enhanced immunity of nanoparticle vaccines. *Expert Rev Vaccines.* 2019;18(3):269-80.
5. **DYKMAN LA.** Gold nanoparticles for preparation of antibodies and vaccines against infectious diseases. *Expert Rev Vaccines.* 2020;19(5):465-77.
6. **FRANÇA A, AGGARWAL P, BARSOV EV, KOZLOV SV, DOBROVOLSKAIA MA, GONZÁLEZ-FERNÁNDEZ Á.** Macrophage scavenger receptor A mediates the uptake of gold colloids by macrophages in vitro. *Nanomedicine.* 2011 Sep;6(7):1175-88.
7. **FABURAY B, RICHT JA.** Short interfering RNA inhibits rift valley fever virus replication and degradation of protein kinase R in human cells. *Front Microbiol.* 2016;7:1889.
8. **MWAENGO D, LORENZO G, IGLESIAS J, WARIGIA M, SANG R, BISHOP RP, ET AL.** Detection and identification of Rift Valley fever virus in mosquito vectors by quantitative real-time PCR. *Virus Res.* 2012;169(1):137-43.
9. **NIKLABSON B, GRANDIEN M, PETERS CJ, GARGAN TP.** Detection of Rift Valley fever virus antigen by enzyme-linked immunosorbent assay. *J Clin Microbiol* 1983;17(6):1026-31.
10. **ZAHER MR, AHMED HA, HAMADA KEZ, TAMMAM RH.** Colorimetric Detection of Unamplified Rift Valley Fever Virus Genetic Material Using Unmodified Gold Nanoparticles. *Appl Biochem Biotechnol.* 2018;184(3):898-908.
11. **RANDALL R, GIBBS CJ, AULISIO CG, BINN LN, HARRISON VR.** The development of a formalin-killed Rift Valley fever virus vaccine for use in man. *J Immunol* 1962;89:660-71.
12. **BONNAFOUS P, NICOLAÏ GM, TAVEAU GHJ, CHEVALIER M, BARRIÈRE F, MEDINA J, ET AL.** Treatment of influenza virus with Beta-propiolactone alters viral membrane fusion. *Biochim Biophys Acta.* 2014;1838(1):355-63.

13. **SUN B, XIA T.** Nanomaterial-Based Vaccine Adjuvants. *J Mater Chem B*. 2016;4(33):5496-509.
14. **CARABINEIRO SAC.** Applications of gold nanoparticles in nanomedicine: Recent Advances in Vaccines. *Molecules*. 2017;22(5):857.
15. **DYKMAN LA, KHLEBTSOV NG.** Immunological properties of gold nanoparticles. *Chem Sci*. 2017;8(3):1719-35.
16. **ABDEL-GAIED HA, HASHEM AE, EL-TAYEB O, MOHAMED AF.** Evaluation of inactivation efficacy of Sabin Polio virus using different inactivating agents and its immunogenicity post nano and microincapsulation. *IJMR* 2010;1(3):114-22.
17. **EL-KARAMANY R, IMAM I, FARID A.** Production of inactivated RVF vaccine. *J Egypt Publ Health Assoc*. 1981;56(5):495-525.
18. World Health Organization. Manual for the laboratory diagnosis of measles and rubella virus infection, 2nd edition, 2007. Visited at: <https://apps.who.int/iris/handle/10665/70211>. Last updated August 2007. Accessed in April 2020.
19. **MARCOLIN E, SAN-MIGUEL B, VALLEJO D, TIEPPO J, MARRONI N, GONZÁLEZ-GALLEGO J, TUÑÓN MJ.** Quercetin treatment ameliorates inflammation and fibrosis in mice with nonalcoholic steatohepatitis. *J Nutr*. 2012 Oct;142(10):1821-8.
20. **BROUCKAERT P, LIBERT C, EVERAERDT B, TAKAHASHI N, CAUWELS A, FIEERS W.** Tumor necrosis factor, its receptors and the connection with interleukin 1 and interleukin 6. *Immunobiology*. 1993;187(3-5):317-29.
21. **DAWSON B, TRAPP RG.** Basic and clinical biostatistics, fourth edition. Lange Medical Books, McGraw Hill, New York, U.S.A. 2004.
22. **DRURY RAB, WALLINGTON EA.** Preparation and fixation of tissues. In: Drury RAB, Wallington EA, editors. *Carleton's Histological Technique*, 5<sup>th</sup> edition. Oxford University Press, New York, United Kingdom, 1980;41-54.
23. **TAN CK, CASTILLO C, SO AG, DOWNEY KM.** An auxiliary protein for DNA polymerase-delta from fetal calf thymus. *J Biol Chem*. 1986;261(26):12310-6.
24. **BANSAL SA, KUMAR V, KARIMI J, SINGH AP, KUMAR S.** Role of gold nanoparticles in advanced biomedical applications. *Nanoscale Adv* 2020;2:3764-87
25. **BAI X, WANG Y, SONG Z, FENG Y, CHEN Y, ZHANG D, ET AL.** The basic properties of gold nanoparticles and their applications in tumor diagnosis and treatment. *Int J Mol Sci*. 2020; 21(7):2480.
26. **TOMIĆ S, ĐOKIĆ J, VASILJIĆ S, OGRINC N, RUDOLF R, PELIGON P, ET AL.** Size-dependent effects of gold nanoparticles uptake on maturation and antitumor functions of human dendritic cells in vitro. *PLoS One*. 2014;9(5):e96584.
27. **SOLIMAN MG, MOHAMED AF, EL SAYED RA, ABO ELQASEM AA.** Immune enhancing potential of sphere and rod gold nanoparticles to rift valley fever vaccine relative to time: in vitro study. *EJBPS*. 2017;4(6):529-36.
28. **AL-OLAYAN ME, MOHAMED FA, EL-KHADRAQY FM, SHEB IR, YEHIA MH.** An Alternative Inactivant for Rift Valley Fever Virus using Cobra Venom-derived L-Amino Oxidase, which is Related to its Immune Potential. *Braz Arch Biol Technol*. 2016;59:e16160044.
29. **EMARA ME, ABDEL-RAHMAN M, MOHAMED FA, NADY S.** Physiological and immunological evaluation of rabies vaccine adsorbed to two different vaccine vehicles. *Egyptian Journal of Medical Microbiology* 2012;21(3):99-110.
30. **ABDELHALIM MAK, MOUSSA SAA, QAID HAY.** The protective role of quercetin and arginine on gold nanoparticles induced hepatotoxicity in rats. *Int J Nanomedicine*. 2018;13:2821-5.
31. **EL SAYED RA, MOHAMED AF.** Assessment of neurological toxicity of gold sphere and rod nanoparticles used as adjuvant to rift valley fever virus vaccine (rvfv) and related physiological changes: in vivo study. *EJBPS* 2017;4(7):112-23.
32. **ABDELHALIM MA, ABDELMOTTALEB MOUSSA SA.** The gold nanoparticle size and exposure duration effect on the liver and kidney function of rats: In vivo. *Saudi J Biol Sci*. 2013;20(2):177-81.
33. **DOUDI M, SETORKI M.** The acute liver injury in rat caused by gold nanoparticles. *Nanomedicine Journal* 2014;1(4):248-57.
34. **NIKURA K, MATSUNAGA T, SUZUKI T, KOBAYASHI S, YAMAGUCHI H, ORBA Y, ET AL.** Gold nanoparticles as a vaccine platform: influence of size and shape on immunological responses in vitro and in vivo. *ACS Nano*. 2013;7(5):3926-38.
35. **CLIMENT N, GARCÍA I, MARRADI M, CHIOFFO F, MIRALLES L, MALENO MJ, ET AL.** Loading dendritic cells with gold nanoparticles (GNPs) bearing HIV-peptides and mannosides enhance HIV-specific T cell responses. *Nanomedicine*. 2018;14(2):339-51.
36. **WEI M, CHEN N, LI J, YIN M, LIANG L, HE Y, ET AL.** Polyvalent immunostimulatory nanoagents with self-assembled CpG oligonucleotide-conjugated gold nanoparticles. *Angew Chem Int Ed Engl*. 2012;51(5):1202-6.
37. **STONE JW, THORNBURG NJ, BLUM DL, KUHN SJ, WRIGHT DW, CROWE JR JE.** Gold nanorod vaccine for respiratory syncytial virus. *Nanotechnology*. 2013;24(29):295102.
38. **LIU Y, JIAO F, QIU Y, LI W, QU Y, TIAN C, ET AL.** Immunostimulatory properties and enhanced TNF- $\alpha$  mediated cellular immunity for tumor therapy by C60 (OH) 20 nanoparticles. *Nanotechnology* 2009; 20(41):415102.

39. **BASTÚS NG, SÁNCHEZ-TILLÓ E, PUJALS S, FARRERA C, KOGAN MJ, GIRALT E, ET AL.** Peptides conjugated to gold nanoparticles induce macrophage activation. *Mol Immunol.* 2009;46(4):743-8.
40. **MALACZEWSKA J.** Effect of oral administration of commercial gold nanocolloid on peripheral blood leukocytes in mice. *Pol J Vet Sci.* 2015;18(2):273-82.
41. **BEKIĆ M, TOMIĆ S, RUDOLF R, MILANOVIĆ M, VUČEVIĆ D, ANŽEL I, ET AL.** The Effect of Stabilisation Agents on the Immunomodulatory Properties of Gold Nanoparticles Obtained by Ultrasonic Spray Pyrolysis. *Materials (Basel).* 2019;12(24):4121.
42. **KOSTELI A, SUBARU E, HAEMMERLE G, MARTIN JF, LEI J, ZECHNER R, ET AL.** Weight loss and lipolysis promote a dynamic immune response in murine adipose tissue. *J Clin Invest.* 2010;120(10):3466-79.
43. **GUO H, ZHANG J, BOUDREAU M, MENG J, YIN JJ, LIU J, ET AL.** Intravenous administration of silver nanoparticles causes organ toxicity through intracellular ROS-related loss of inter-endothelial junction. *Part Fibre Toxicol* 2016;13:21.
44. **SADAUSKAS E, WALLIN H, STOLTENBERG M, VOGEL U, DOERING P, LARSEN A, ET AL.** Kupffer cells are central in the removal of nanoparticles from the organism. *Part Fibre Toxicol* 2007;4(1):1-7.
45. **ABDELHALIM MAK, JARRAR BM.** Histological alterations in the liver of rats induced by different gold nanoparticle sizes, doses, and exposure duration. *J Nanobiotechnology* 2012;10:5.
46. **PATLOLLA AK, KUMARI SA, TCHOUNWOU PB.** A comparison of poly-ethylene-glycol-coated and uncoated gold nanoparticle-mediated hepatotoxicity and oxidative stress in Sprague Dawley rats. *Int J Nanomedicine.* 2019;14:639-47.
47. **ABDELHALIM MAK.** Exposure to gold nanoparticles produces pneumonia, fibrosis, chronic inflammatory cell infiltrates, congested and dilated blood vessels, and hemosiderin granule and emphysema foci. *J. Cancer Sci Ther.* 2012;4(3):46-50.
48. **IBRAHIM KE, AL-MUTARY MG, BAKHIET AD, KHAN HA.** Histopathology of the liver, kidney, and spleen of mice exposed to gold nanoparticles. *Molecules* 2018;23(8):1848.
49. **NIIKURA K, MATSUNAGA T, SUZUKI T, KOBAYASHI S, YAMAGUCHI H, ORBA Y, ET AL.** Gold nanoparticles as a vaccine platform: influence of size and shape on immunological responses in vitro and in vivo. *ACS Nano.* 2013;7(5):3926-38.
50. **HWANG JH, KIM SJ, KIM YH, NOH JR, GANG GT, CHUNG BH, LEE CH.** Susceptibility to gold nanoparticle-induced hepatotoxicity is enhanced in a mouse model of nonalcoholic steatohepatitis. *Toxicology* 2012;294(1):27-35.
51. **ABDELHALIM MAK, JARRAR BM.** Gold nanoparticles induced cloudy swelling to hydropic degeneration, cytoplasmic hyaline vacuolation, polymorphism, binucleation, karyopyknosis, karyolysis, karyorrhexis and necrosis in the liver. *Lipids Health Dis.* 2011;10:166.
52. **MULLER AP, FERREIRA GK, DA SILVA S, NESI RT, DE BEM SILVEIRA G, MENDES C, ET AL.** Safety protocol for the gold nanoparticles administration in rats. *Mater Sci Eng C Mater Biol Appl.* 2017;77:1145-50.
53. **FRAGA S, BRANDÃO A, SOARES ME, MORAIS T, DUARTE JA, PEREIRA L, ET AL.** Short-and long-term distribution and toxicity of gold nanoparticles in the rat after a single-dose intravenous administration. *Nanomedicine.* 2014;10(8):1757-66.
54. **KABIR N, ALI H, ATEEQ M, BERTINO MF, SHAH MR, FRANZEL L.** Silymarin coated gold nanoparticles ameliorate CCl<sub>4</sub>-induced hepatic injury and cirrhosis through down regulation of hepatic stellate cells and attenuation of Kupffer cells. *RSC Adv* 2014;4(18):9012-20.
55. **BAHARARA J, RAMEZANI T, DIVSALAR A, MOUSAVI M, SEYEDARABI A.** Induction of apoptosis by green synthesized gold nanoparticles through activation of caspase-3 and 9 in human cervical cancer cells. *Avicenna J Med Biotechnol.* 2016;8(2):75-83
56. **TIAN F, GLIFT MJ, CASEY A, DEL PINO P, PELAZ B, GONDE J, ET AL.** Investigating the role of shape on the biological impact of gold nanoparticles in vitro. *Nanomedicine* 2015;10(17):2643-57.
57. **SELIM ME, HENDI AA.** Gold nanoparticles induce apoptosis in MCF-7 human breast cancer cells. *Asian Pac J Cancer Prev.* 2012;13(4):1617-20.
58. **REN KW, LI YH, WU G, REN JZ, LU HB, LI ZM, ET AL.** Quercetin nanoparticles display antitumor activity via proliferation inhibition and apoptosis induction in liver cancer cells. *Int J Oncol.* 2017;50(4):1299-311.
59. **CHO WS, CHO M, JEONG J, CHOI M, CHO HY, HAN BS, ET AL.** Acute toxicity and pharmacokinetics of 13 nm-sized PEG-coated gold nanoparticles. *Toxicol Appl Pharmacol.* 2009;236(1):16-24
60. **KUANG H, YANG P, YANG L, AGUILAR ZP, XU H.** Size dependent effect of ZnO nanoparticles on endoplasmic reticulum stress signaling pathway in murine liver. *J Hazard Mater.* 2016;317:119-26.
61. **WANG S, LIU H, ZHANG X, QIAN F.** Intranasal and oral vaccination with protein-based antigens: advantages, challenges and formulation strategies. *Protein Cell.* 2015;6(7):480-503.
62. **ALFRANCA G, BEOLA L, LIU Y, GUTIÉRREZ L, ZHANG A, ARTIGA A, ET AL.** In vivo comparison of the biodistribution and long-term fate of colloids-gold nano prisms and nanorods-with minimum surface modification. *Nanomedicine* 2019;14(23):3035-55.

63. **POORNIMA K, AARON GA, VIVEK G, KAPIL P, BALABHASKAR P, ERKKI R, ET AL.** Using shape effects to target antibody-coated nanoparticles to lung and brain endothelium. *Proc Natl Acad Sci USA*. 2013; 110(26):10753-8.
64. **BLACK KC, WANG Y, LUEHMANN HP, CAI X, XING W.** Radioactive <sup>198</sup>Au-doped nanostructures with different shapes for in vivo analyses of their bio distribution, tumor uptake, and intratumoral distribution. *ACS Nano*. 2014;8(5):4385-94.
65. **BARTUCCI R, PARAMANANDANA A, BOERSMA YL, OLINGA P, SALVATI A.** Comparative study of nanoparticle uptake and impact in murine lung, liver and kidney tissue slices. *Nanotoxicology*. 2020; 14(6):847-65.
66. **COLINO CI, LANA O JM, GUTIERREZ-MILLAN C.** Targeting of hepatic macrophages by therapeutic nanoparticles. *Front Immunol*. 2020;11:218.
67. **SÖDERSTJERNA E, BAUER P, CEDERVALL T, ABDSHILL H, JOHANSSON F, JOHANSSON UE.** Silver and gold nanoparticles exposure to in vitro cultured retina—studies on nanoparticle internalization, apoptosis, oxidative stress, glial-and microglial activity. *PLoS One* 2014;9(8):e105359.